Experimental Research

ANNALS OF MEDICINE & SURGERY

OPEN

# Transplantation of acellular amniotic membrane seeded with adipose-derived mesenchymal stem cells in a rat model of intrauterine adhesion

Chunbo Li, MD, PhD[a], Liangfeng Yao[b], Fengquan He[c,*], Keqin Hua, MD, PhD[a,*]

**Objective:** This study aimed to investigate the role of acellular amniotic membrane (AAM) loaded with adipose-derived mesenchymal stem cells (ADSCs) for the treatment of intrauterine adhesion.

**Methods:** One hundred twenty female Spargue-Dawley rats were randomly divided into four groups: sham operation group (the uterus was picked out and incised without treatment), intrauterine adhesion group, the experimental group treated with AAM, and experimental group treated with AAM loaded with ADSCs. Histological and immunohistochemical analysis were performed on 3, 7, and 14 days after surgery to evaluate the degree of uterine fibrosis and regeneration of injured endometrium. RNA sequencing and real-time PCR were used to explore the potential mechanism by which ADSCs modulated immune response and promoted endometrial regeneration.

**Results:** On 14 days after surgery, the endometrial thickness, number of glands, and degree of fibrosis reduction in the ADSCs/AAM group was higher than those in the AAM group, and similar to the sham operation group. RNA sequencing analysis showed that ADSCs can modulate local immune responses and promote the formation of functional endometrium. Meanwhile, we found that ADSCs significantly decreased the levels of pro-inflammatory cytokines (TNF-α and IL-1β) and increased the levels of anti-inflammatory cytokines (bFGF and IL-6).

**Conclusion:** Our results demonstrated that AAM loaded with ADSCs can result in the regeneration of injured endometrium and fibrosis reduction. Meanwhile, ADSCs also regulated the immune microenvironment, which was beneficial to functional endometrial recovery.

**Keywords:** acellular amniotic membrane, intrauterine adhesions, regeneration, stem cells, tissue engineering

## Introduction

The characteristic of IUA is the formation of fibrosis, where the adhesive tissue partially or completely occludes the uterine cavity due to various damage to the basal layer of the endometrium[1,2]. It often leads to menstrual abnormalities, secondary infertility, and recurrent miscarriage, which is a serious reproductive health problem[3]. Although various clinical methods have been used to reconstruct the anatomical structure of the uterine cavity and promote the recovery of functional endometrium, including hysteroscopic adhesiolysis, hormonal treatment, or the placement of barriers (e.g. barrier gels and intrauterine devices), the high risk of re-adhesion after resection is still a major challenge[4].

In order to prevent adhesion recurrence and promote endometrial regeneration, the application of tissue engineering provides a new therapeutic strategy[5]. Human amniotic membrane (hAM) is a natural high-molecular biological material composed of the basal membrane, avascular collagen stroma, monolayer epithelial cells, and underlying fibroblasts. hAM contains various

### HIGHLIGHTS

- We investigated the potential role of acellular amniotic membrane (AAM) loaded with adipose-derived mesenchymal stem cells (ADSCs) in preventing intrauterine adhesion (IUA) after endometrial injury.
- Our results indicated that ADSCs/AAM can promote endometrial regeneration by measuring endometrial thickness, gland numbers, and vascular area.
- Our results indicated that the transplantation of ADSCs can provide a suitable environment for endometrial regulation.
- Our results indicated that ADSCs can regulate the inflammatory response.

[a]Department of Obstetrics and Gynecology, The Obstetrics & Gynecology Hospital of Fudan University, Shanghai, [b]Department of Obstetrics and Gynecology, Zhangzhou Municipal Hospital of Fujian Province, Zhangzhou and [c]Department of Obstetrics and Gynecology, Maternal and Child Health Hospital of HongHe Hani and Yi Autonomous Prefecture, Yunnan, China

C.L. and L.Y. contributed equally to this study.

Sponsorships or competing interests that may be relevant to content are disclosed at the end of this article.

*Corresponding author. Address: Department of Obstetrics and Gynecology, The Obstetrics & Gynecology Hospital of Fudan University, 419 FangXie Road, Shanghai 200011, China. Tel.: +21 331 899 00. E-mail: huakeqinjiaoshou@163.com (K. Hua); Department of Obstetrics and Gynecology, Maternal and Child Health Hospital of HongHe Hani and Yi Autonomous Prefecture, 1 Qiyuan Road, Gejiu City, Yunnan Province 661199, China. Tel.: +87 321 226 06. E-mail:hhzfyyhfq@126.com (F. He).



Annals of Medicine & Surgery (2024) 86:4463–4474

Received 5 December 2023; Accepted 27 May 2024

Published online 1 July 2024

http://dx.doi.org/10.1097/MS9.0000000000002249

growth factors and extracellular matrix (ECM) components, which are beneficial for cell growth and proliferation. The human acellular amniotic membrane (hAAM) scaffolds were derived from hAM by removing the cellular components of fresh hAM, and have been successfully applied to tissue regeneration[6]. AAM, as a biocompatible biomaterial, has beneficial effects on the recovery of blood vessels, cartilage, urinary tract epithelium, genitourinary tract, larynx, and stomach[6]. Many advantageous characteristics of AAM, such as availability, inexpensiveness, and ease of isolation, make it a potential biomaterial for tissue engineering, especially in skin and soft tissue engineering[7,8]. Recently, some studies have reported the value of AAM in reducing IUAs and promoting endometrial regeneration[9]. ADSCs are precursor cells that have been shown to secrete various bioactive molecules, such as growth factors, cytokines, and chemokines[10,11]. Several studies have also reported that ADSCs can be recruited to the site of endometrial injury, where they differentiate into endometrial cells and promote angiogenesis, resulting in better pregnancy outcomes[12–14]. However, the problem is that due to the lack of supportive scaffolds, stem cells often migrate to other locations after in-situ injection. Therefore, in order to solve the problem of limited cell transplantation, suitable materials should be used as carriers to provide support for cell transplantation.

In this study, hAAM was used as a scaffold to provide support and prevent the spread of ADSCs. This study aimed to evaluate the feasibility and effectiveness of hAAM loaded with ADSCs in reducing intrauterine fibrosis and promoting the regeneration of damaged endometrium and to explore the potential mechanisms by which ADSCs regulate the immune microenvironment (Fig. 1).

## Materials and methods

### *Animals*

A total of 120 female Sprague-Dawley rats, weighing 220–240 g were purchased from Silaike Corporation (Shanghai, China) and housed four to five per cage in a controlled environment that was maintained at 22°C with 12 h light/dark cycles. Food and water were available ad libitum. Ethical approval for this study (number: 2021JS-017) was proven by the ethical committee of our hospital in December 2022. The work has been reported in line with the ARRIVE criteria[15].

### *Culture, identification, and multilineage differentiation of adipose-derived mesenchymal stem cells*

Rat subcutaneous inguinal fat was collected, chopped manually, and digested with equal amounts of phosphate-buffered saline (Falcon, USA), supplemented with 0.075% type I collagenase (Washington Biochemical Corp., USA), and then gently shaped at 37°C for 60 min. After enzyme neutralization, the digested tissue was centrifuged at 2000 g for 10 min and filtered through double-layer gauze to remove large debris. The pellets were resuspended in LG-MEM containing 10% FBS, 100 µg/ml streptomycin, and 100 U/ml penicillin solution and plated in 100 mm culture dishes (Falcon). After reaching 70–80% confluency, the cells were passed on to the next generation for further experiments. ADSCs were identified by the cell surface antigens CD45, CD90, CD11, CD44, and CD29, using flow cytometry assays. The multilineage differentiation of ADSCs was examined by adipogenic, osteogenic, and chondrogenic differentiation assays. Adipogenesis was induced by adipogenic induction medium (Gibco) for 14 days, and intracellular lipid accumulation was confirmed by Oil red O

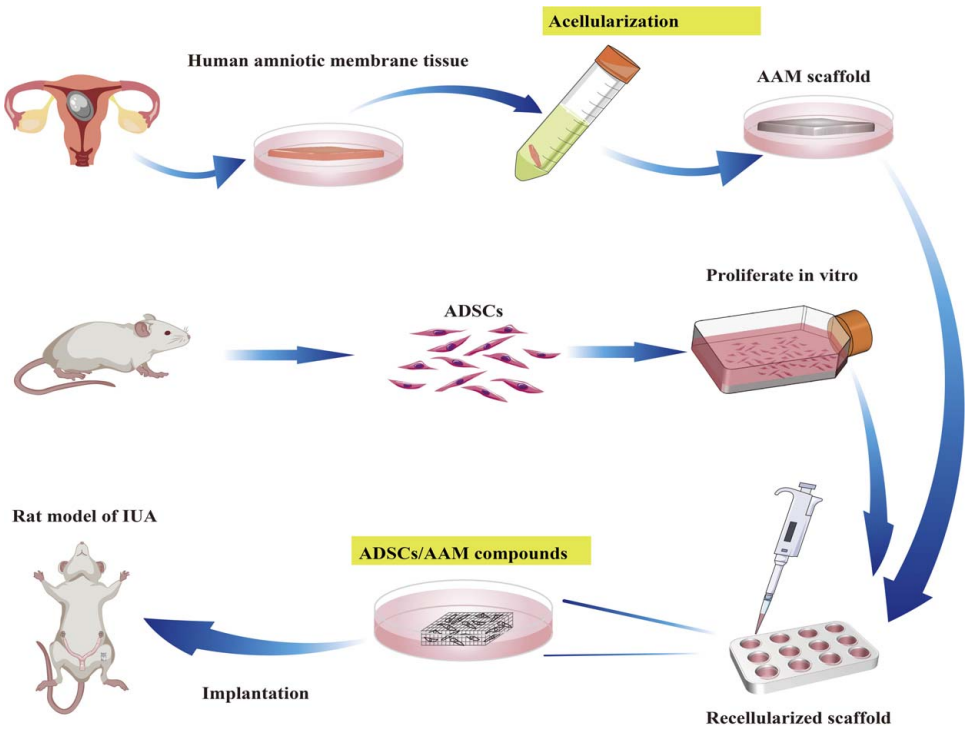


**Figure 1.** A brief schematic diagram of the experimental design.

staining. Osteogenesis was induced by an osteogenic induction medium (Gibco) for 21 days, and calcium deposition was shown by alizarin-red staining. Chondrogenic differentiation was induced with a chondrogenic induction medium (Gibco) for 28 days and identified by toluidine blue staining. The use of stem cells was referred to the International Society for Stem Cell Research (ISSCR) guidelines (https://www.isscr.org/guidelines)[16].

### Preparation of human acellular amniotic membrane

After obtaining approval from the ethics committee of our hospital for the use of the hAM, fresh hAM was obtained from healthy patients after natural delivery or cesarean section procedures under sterile conditions. The donors were between 25 and 35 years old and had no history of membrane rupture, endometritis, meconium obstruction, HIV-1/2, hepatitis B, hepatitis C, human T-cell lymphovirus, syphilis, cytomegalovirus, and tuberculosis. All participants completed informed consent. Then, the preparation of AAM was based on the report by Koizumi *et al.*[17]. Briefly, fresh hAM was mechanically separated from the chorionic membrane and then thawed prior to decellularization. After washing three times with 0.9% NaCl solution to remove blood and cellular debris, hAM was incubated with 0.02% ethylenediaminetetraacetic acid solution at 37°C for 2 h, with continuous agitation for decellularization. Then, the membrane was decellularized in a devitalization buffer containing 0.25% N-ethylmaleimide (Sigma-Aldrich) and 2% N-lauryl sarcosine (Sigma) at room temperature. The devitalization solution was removed and replenished every 4 h, for a total of 12 h. After dialysis, the acellular hAM was lyophilized overnight and subsequently sterilized overnight with ethylene oxide gas and then stored at 4°C. The surface morphology and structure of the hAAM scaffolds were evaluated using scanning electron microscopy (SEM; Hitachi, Tokyo, Japan; S4800).

### The construction of adipose-derived mesenchymal stem cells/acellular amniotic membrane compounds

Before implantation, the AAM was cut into $2 \times 0.5$ cm pieces and soaked in normal saline for 10 min. ADSCs at passage 3 were resuspended in the culture medium at a density of $5 \times 10^5$/ml. Hundred microliters of cell suspension were evenly seeded in AAM to infiltrate the cell surface. After cells were incubated at 37°C for 4 h to allow cells to adhere to the membrane, a growth medium was added to continue the incubation. After 24 h of incubation, the ADSCs/AAM constructs were transferred to new wells for subsequent in vitro culture. One week after implantation, the deposition of ADSCs on AAM was examined by SEM. Samples were then mounted, sputter-coated with gold, and viewed by SEM to observe adhesion and ECM deposition under the surface of AAM. In addition, on 3 and 7 days after implantation, the viability of ADSCs on AAM was evaluated using a live/dead cell staining kit (Biovision, USA). Briefly, ADSCs/AAM constructs were washed with phosphate-buffered saline and incubated in assay reagents (2 μM calcein AM and 4 μM ethidium homodimer-1) for 15 min. Then, the stained live and dead cells were detected by confocal laser microscopy with a band-pass filter (FITC and rhodamine). Live cells showed green fluorescence, while the nuclei of dead cells were stained red.

### Surgical procedure

The rat IUA model was established using the mechanical injury method. Briefly, rats were anesthetized by intramuscular injection of 10% chloral hydrate 300 mg/kg, and the abdominal cavity was opened after disinfection with iodophor. There were no rats presenting signs of peritonitis. Then, the uterus was slowly picked out and incised 2 cm from the upper one-third of the upper uterus. The endometrial tissue was then scraped to the depth of the muscular layer. In the ADSCs/AAM group, the ADSCs/AAM constructs were introduced to cover the damaged area. In the AAM group, AAM was placed at the lesion of the uterine. In the IUA group, the lesion was sutured directly to achieve self-healing. In the sham operation group, the uterus was exposed to air for 20 min after opening the abdomen. Finally, the uterus was closed with 6-0 absorbable suture intermittently. After washing the abdominal cavity with saline, the rectus fascia and skin were sutured with 4-0 silk suture. On 3, 7, and 14 days after surgery ($n = 12$, 12 uteri at each time point), the rats were sacrificed under deep anesthesia (5% isoflurane) by exsanguination, and the entire uterus was dissected and sectioned transversely for further evaluation.

### Histological examination and immunohistochemical staining

After fixing the uterine tissue with 4% paraformaldehyde and embedding it in paraffin, the samples were cut into 4–6 μm sections for H&E and Masson's trichrome staining. A light microscope was used to counter-view morphological changes. Five areas in each image were selected for counting. Image Pro-Plus 6.0 was applied to analyze endometrial thickness, total number of endometrial glands, and fibrotic area. For immunohistochemistry staining, samples were tested for CD31, GB13063, 1:200, Servicebio, (an indicator of endothelial cells of microvessels), vimentin, ab92547, 1:200, abcam, (a marker of stromal cells), VEGF, ab32152, 1:200, abcam, (a vascular marker) and E-cadherin, sc-8426 1:50, Santa Cruz, (a marker of epithelial cells).

### Next-generation RNA sequencing and bioinformatics analysis

Total RNA was extracted from four groups of the whole uterus on 3 and 14 days after surgery using TRIzol according to the manufacturer's protocol (Invitrogen). The Illumina standard kit was used according to the TruSeq RNA SamplePrep Guide (Illumina). Magnetic beads containing oligo (dT) were used to isolate poly(A) mRNA from total RNA. Purified mRNA was then fragmented. Using these short fragments as templates, first-strand complementary DNA (cDNA) was synthesized using random hexamer primers and reverse transcriptase (SuperScript II, Invitrogen). Second-strand cDNA was synthesized using buffer, dNTPs, RNase H, and DNA polymerase I. Short double-stranded cDNA fragments were purified using the QIAquick PCR Extraction Kit (Qiagen) and eluted with EB buffer for end repair and the addition of an 'A' base. The short fragments were ligated to the Illumina sequencing adapters. DNA fragments of selected size were gel-purified with a QIAquick PCR extraction kit (Qiagen) and amplified by PCR. The library was then sequenced on an Illumina HiSeq 2000 sequencing machine. The library size was 400 bp, the read length was 116 nt, and the sequencing strategy was paired-end sequencing. Clean reads were used for subsequent analysis and were mapped to the reference genome by

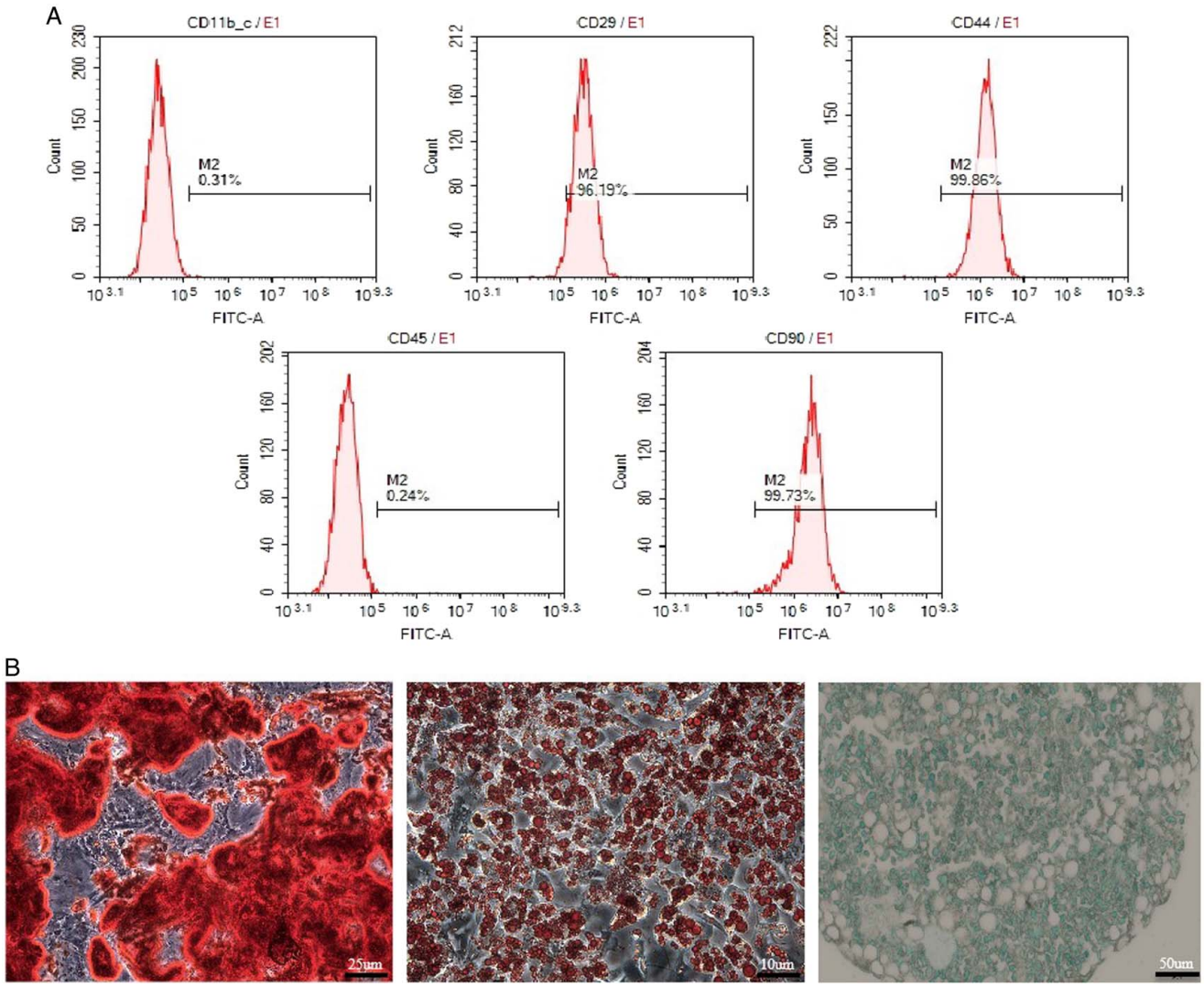


**Figure 2.** Characteristics of adipose-derived stem cells (ADSCs). (A) FACS analysis showing the expression of common surface markers of stem cells, CD11b/c, CD29, CD44, CD45 and CD90. (B) These three classic tests of stem cells were present. Osteogenic induction, adipogenic induction, and chondrogenic induction of ADSCs.

TopHat. The gene expression was measured by the number of uniquely mapped fragments per kilobase of exon per million mapped fragments. The R package 'limma' was used to create differential expression genes. The Database for Annotation, Visualization, and Integrated Discovery (DAVID) bioinformatics resource was used to annotate gene function and pathway.

### *RNA isolation and polymerase chain reactions*

In order to investigate the regulation effect of ADSCs on inflammatory response, we performed real-time PCR. According to the manufacturer's protocol, RNAprep Micro Kit (TianGen Biotech, Beijing, China) was used to extract total RNA. Total RNA samples were extracted from excised uterine horns with RNAiso Plus (Takara Bio) and dissolved in water treated with diethylpyrocarbonate. RNA concentrations were quantified using NanoDrop 2000 spectrophotometery (NanoDropTechnologies, Thermo Scientific). Two micrograms total RNA was reverse-transcribed into cDNA in a 20 μl reverse transcription system with the Primestar extaq cDNA Synthesis Kit (TaKaRa). The reactions were performed and monitored in a T3 thermocycler (Biometra). Real-time PCR was performed using a quantitative real-time amplification system (MxPro-Mx3000P; Stratagene, La Jolla, CA, USA). SybrGreen PCR MasterMix (Applied Bio-systems, Foster City, CA, USA) was used in each reaction. To compare transcription levels of target genes in different quantities of sample, the quantified cDNA transcript level (cycle threshold) to that of GAPDH was used for normalization of real-time PCR results. Each sample was assayed three times.

### *Fertility test*

The function of the uterine horns was assessed by testing their ability to receive fertilized ova and supporting embryos to the late stage of pregnancy. On 28 days after transplantation, another subset of rats from each group ($n = 6$, with 12 uterine horns) was mated with fertile male rats. Rats were euthanized 14 days after the presence of the vaginal plugs, and each uterine horn was examined for the number, size, and weight of fetuses, as well as the site of implantation.

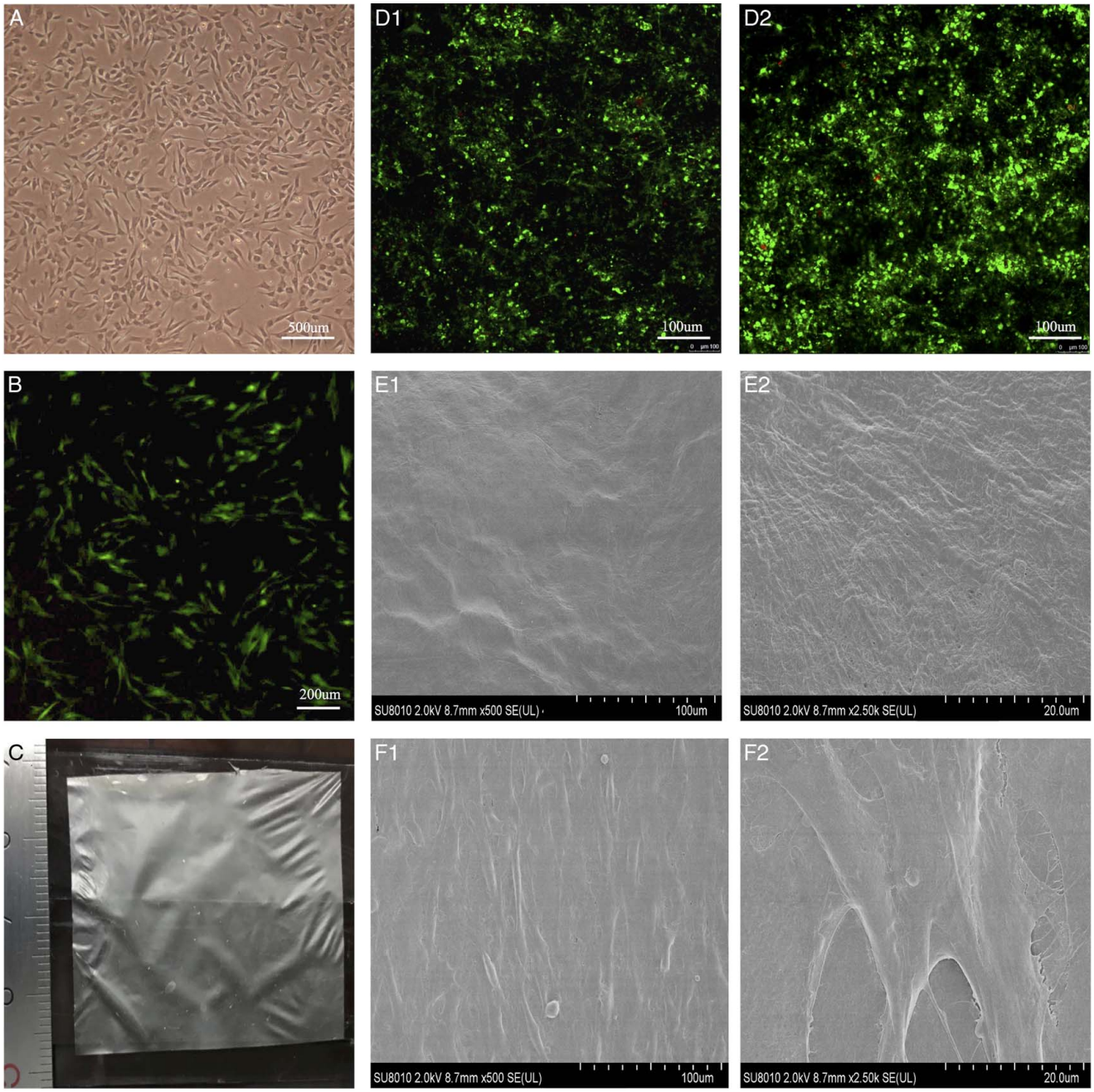


**Figure 3.** Implantation of adipose-derived stem cells (ADSCs) on acellular amniotic membrane (AAM). (A) Representative image of ADSCs. Scale bar = 500 μm, Scale bar = 100 μm; (B) ADSCs labeled using Dil, Scale bar = 200 μm; (C) Gross view of AAM; (D1, D2) live/dead staining of ADSCs on the scaffolds after 3 and 14 days; (E1, E2) Representative images of AAM and (F1, F2) AAM implanted with ADSCs by SEM. Scale bar = 200 μm.

### *Tracing of adipose-derived mesenchymal stem cells in vivo*

Dil is a nontoxic fluorescent marker of cell membranes that is used to track implanted cells. ADSCs were labeled with Dil (Sigma-Aldrich, St Louis, MO, USA)[18]. After washing, stained cells were cultured in sterile phosphate-buffered saline. Dil-labeled ADSCs were then resuspended in the culture medium at a density of $5 \times 10^5$/ml and seeded on AAM scaffolds to form ADSCs/AAM compounds, which were implanted in the injured uterine. On days 3, 7, and 14 after implantation, rats were sacrificed, and uterine tissues were collected and frozen at – 80 °C. Frozen tissues were continuously cut into 4-μm sections, and the nucleus was stained with DAPI. The samples were then observed by fluorescence microscopy (magnification × 100, Olympus).

### *Statistical analysis*

All data are reported as means ± SD analyzed by SPSS 20.0. Statistical analysis was performed by Student's *t* test for comparisons of different groups. A *P* value less than 0.05 was considered statistically significant.

## Results

### *Characteristics of adipose-derived mesenchymal stem cells, acellular amniotic membrane and adipose-derived mesenchymal stem cells/acellular amniotic membrane*

ADSCs were cultured to the third generation. FACS analysis showed that the expression levels of ADSCs surface markers CD29, CD44, and CD90 were 96.19, 99.86, and 99.73%, respectively, while the expression levels of hematopoietic stem cell markers CD11b and CD45 were 0.31 and 0.24%, respectively (Fig. 2A). Osteogenesis, adipogenesis, and chondrogenic differentiation were confirmed by Alizarin-Red staining, Oil red O staining, and Toluidine blue staining, respectively (Fig. 2B). ADSCs exhibited a fibroblast-like morphology (Fig. 3A). The fluorescence microscope revealed the shape of ADSCs pre-labeled with the fluorescent dye Dil (Fig. 3B). AAM exhibited a thin-film structure that can be easily tailored into various shapes to fill defect (Fig. 3C). Live/dead staining showed that ADSCs could continue to proliferate without apoptosis (Fig. 3D1 and D2). SEM showed collagen fibers on AAM (Fig. 3E1 and E2), while abundant ECM deposition was observed on the ADSCs/AAM compounds (Fig. 3F1 and F2).

### *Regeneration of injured endometrium*

To evaluate the value of ADSCs and AAM in the treatment of IUA, we applied ADSCs/AAM or AAM to a rat model of IUA. The endometrial surface in the sham operation group was covered by highly columnar epithelial cells 14 days after surgery. In the ADSCs/AAM group, HE staining showed intact endometrial layer structure and normal epithelial cells, similar to the sham operation group. In addition, the endometrial thickness and number of glands in the ADSCs/AAM group were higher than those in the AAM group. However, in the IUA group, the endometrial layer was destroyed, and the uterine cavity was filled with fibrous tissue (Figs 4 and 5).

To evaluate the degree of endometrial fibrosis, we performed Masson staining on collagen fibers. In the sham operation group, there was almost no collagen deposition in the endometrial stroma. Compared to the sham operation group, the collagen deposition in the IUA group was significantly increased. However, on 14 days after surgery, the incidence of endometrial fibrosis in the ADSCs/AAM group was significantly reduced compared to the IUA group (Figs 4 and 5).

Then, 14 days after surgery, we performed immuno-expression of CD31, VEGF, vimentin, and E-cadherin in all groups (Fig. 6). CD31 is a marker of endothelial cells in the stroma and can be used to measure the microvascular density[19]. VEGF is a well-known angiogenic factor in the cytoplasm and is crucial for neovascularization[20]. Our results showed that the microvascular density of the ADSCs/AAM group was significantly higher than that of the AAM group, similar to the sham operation group. The administration of ADSCs resulted in a slightly high expression of VEGF, similar to the expression of VEGF in the sham operation group. Vimentin is a marker of stromal cells and is mainly expressed in the cytoplasm of endometrial stromal cells[21]. Compared with the AAM group, the expression of vimentin in the ADSCs/AAM group was similar to that in the sham operation group. E-cadherin is a transmembrane protein expressed in epithelial cells and plays an important role in maintaining the stability of epithelial cells[22]. The expression of

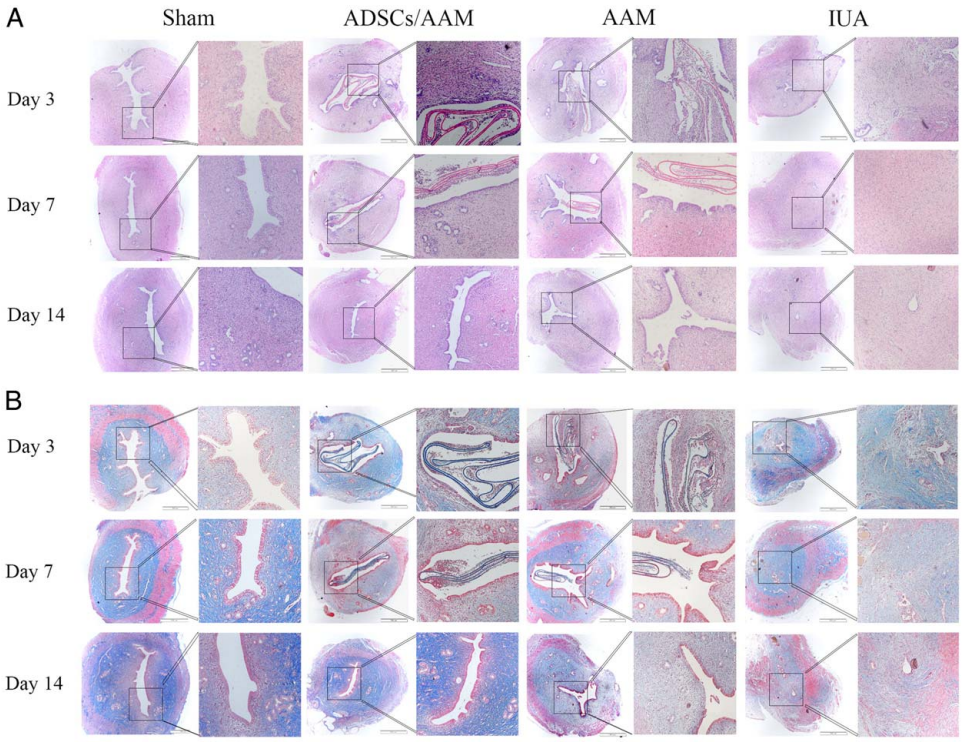


**Figure 4.** Histopathological characteristics were tested by H&E staining (A), and Masson trichrome staining (B), on 3, 7, and 14 days after surgery in sham, ADSCs/AAM, AAM, and IUA group. Scale bar = 200 μm. Scale bar = 50 μm. AAM, acellular amniotic membrane; ADSC, adipose-derived stem cells; IUA, intrauterine adhesion.

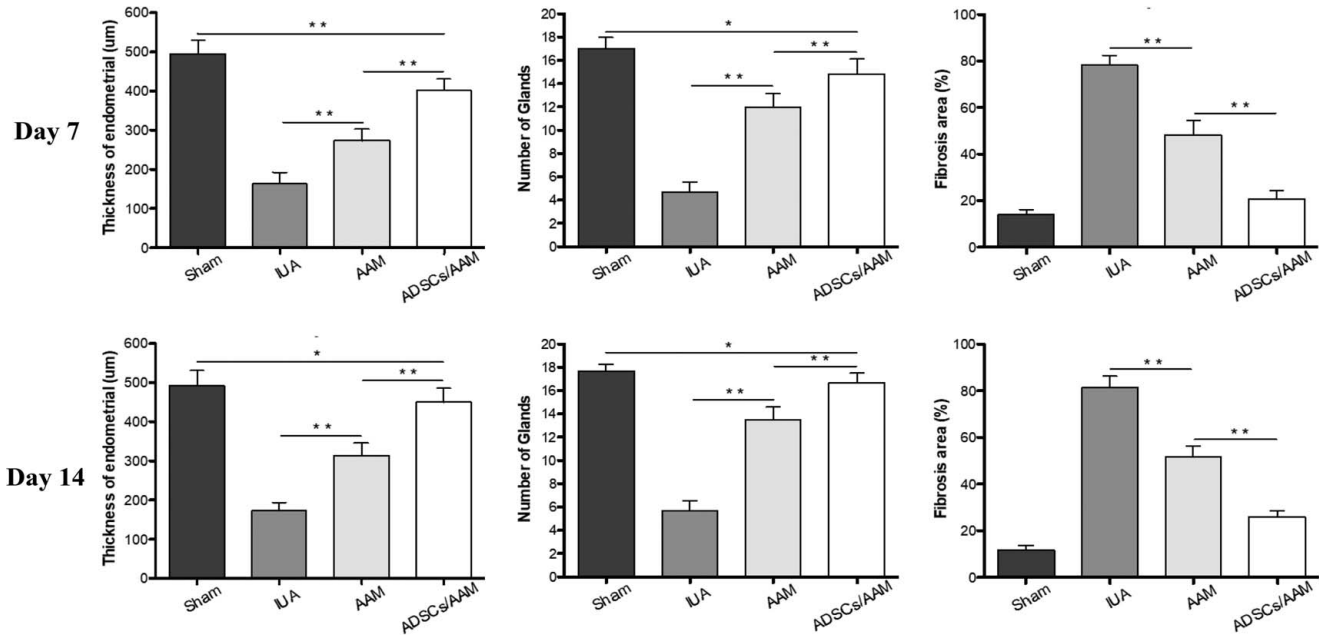


**Figure 5.** Scoring of thickness of endometrium, number of glands and fibrosis area according to histopathological images on 7 and 14 days after surgery in the sham operation, ADSCs/AAM, AAM and IUA group. *$P$ value $>0.05$ and **$P$ value $<0.05$. All results are showed as the mean ± SD of three independent experiments. AAM, acellular amniotic membrane; ADSC, adipose-derived stem cell; IUA, intrauterine adhesion.

E-cadherin in the ADSCs/AAM group was significantly higher than that in the AAM group (Fig. 6).

Finally, we also tested 24 IUA models in 12 rats for pregnancy at 4 weeks after transplantation with or without ADSCs/AAM (Fig. 7A). In the sham operation group, four uteruses conceived (66.7%), and no cases in the IUA group. In the ADSCs/AAM group, although three uteruses were conceived (50%), the average number of embryos per uterus was one to two embryos, compared to three to four embryos in the sham operation group (Fig. 7B). On the contrary, ADSCs/AAM led to an improvement trend in fertility recovery, with a pregnancy rate of 50% and 1 ± 2 gestational embryos.

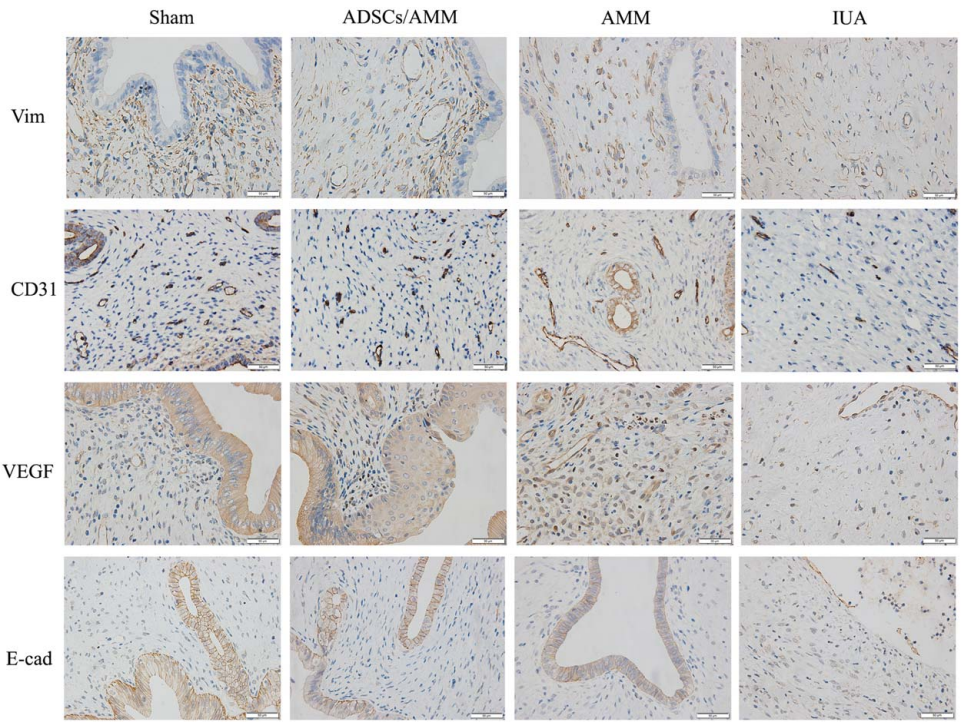


**Figure 6.** Immunohistochemical staining of CD31, VEGF, vimentin, and E-cadherin on 14 days postoperatively. Scale bar = 50 μm.

### *The regulatory effect of stem cells on inflammatory response*

In order to further explore the regulatory mechanism of ADSCs in the process of endometrial repair, we performed RNA sequencing on uterine tissue 3 and 14 days after surgery. Our results showed high expression levels of COL4A1, MSN, and HMOX1 in the IUA group 3 days after surgery (Fig. 8A), and GO analysis showed high enrichment in endothelial development, lymphangiogenesis, and leukocyte migration (Fig. 8C). On 14 days after surgery, the levels of COL3A1, COL1A1, and ACTG2 expression in the IUA group was high, and GO analysis showed high enrichment of ECM organization, cell-substrate adhesion, endodermal cell differentiation, and leukocyte migration. These results indicated that the formation of stable fibrous tissue covered the damaged endometrium. Then, we evaluated the effect of ADSCs on fibrosis formation and endometrial regeneration. Not surprisingly, on 3 and 14 days after surgery, the levels of SPP1, LYZ2, APOE, and CTSB expression in the ADSCs/AAM group were higher compared to the sham operation group (Fig. 8B). In the early phase, GO analysis showed high enrichment of antigen processing, leukocyte chemotaxis, phagocytosis, neutrophil activation, and endocytosis (Fig. 8D), indicating that ADSCs could exert immunomodulatory effects. In the late phase (14 days after surgery), GO analysis revealed normal functional enrichment in the ADSCs/AAM group, including ribosome, protein targeting, and RNA catabolic process (Fig. 8D). Then, we evaluated the expression of inflammatory cytokines (bFGF, IL-1β, IL-6, and TNF-α1) (Fig. 9). The results showed that the level of anti-inflammatory cytokines, such as bFGF and IL-6 in the ADSCs/AAM group, were significantly increased on 3 and 7 days after surgery compared to the AAM group. Meanwhile, the level of pro-inflammatory cytokines, such as TNF-α and IL-1β in the ADSCs/AAM group, was significantly decreased on 3 and 7 days after surgery compared to the AAM group. However, there were no significant differences in both anti-inflammatory and pro-inflammatory cytokines between the ADSCs/AAM and AAM groups on 14 days after surgery.

### *The tracing of stem cells in vivo*

ADSCs were labeled with Dil, a flourochrome used to track living cells in vivo. On 3, 7, and 14 days after surgery, a fluorescent microscope revealed that Dil-labeled ADSCs were distributed near the damaged endometrium and had incorporated into endometrium tissue. The signal attenuated but was still present 14 days after surgery (Fig. 10).

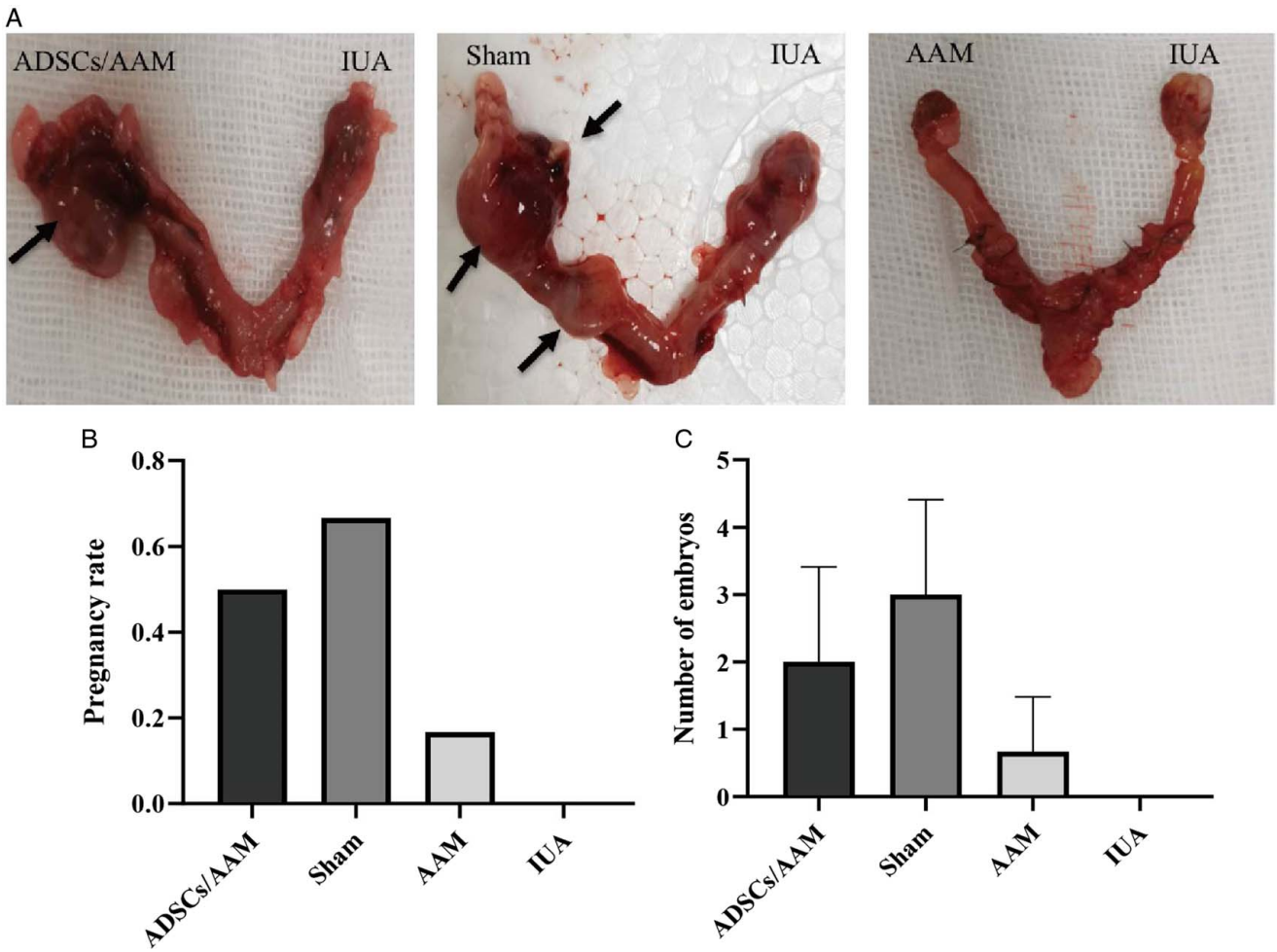


**Figure 7.** Evaluation of fertility restoration. Representative pictures of uterine horns after 14 days of confirmed mating by vaginal plug (A); pregnancy rate after 14 days of confirmed mating by vaginal plug (B); number of gestational sacs after 14 days of confirmed mating by vaginal plug (C).


**Figure 8.** Heatmap of expression profiles of top 10 differently expressed genes (DEGs) between IUA and sham group at 3 (left) and 14 days (right) after surgery (A); Heatmap of expression profiles of top 10 differently genes between ADSCs/AAM and AAM group at 3 (left) and 14 days (right) after surgery (B); comparison of functional enrichment between IUA and sham group on 3 (left) and 14 days (right) after surgery (C); comparison of functional enrichment between ADSCs/AAM and AAM group on 3 (left) and 14 days (right) after surgery (D). AAM, acellular amniotic membrane; ADSC, adipose-derived stem cell; IUA, intrauterine adhesion.

## Discussion

IUA usually occurs when the endometrium fails to regenerate and is replaced by fibrotic tissue[2,3]. Therefore, the ideal treatment method must simultaneously prevent the formation of fibrosis and promote endometrial regeneration. In this study, we investigated the potential role of AAM loaded with ADSCs in preventing IUA after endometrial injury. Our results indicated that ADSCs/AAM can promote endometrial regeneration by measuring endometrial thickness, gland numbers, and vascular area.

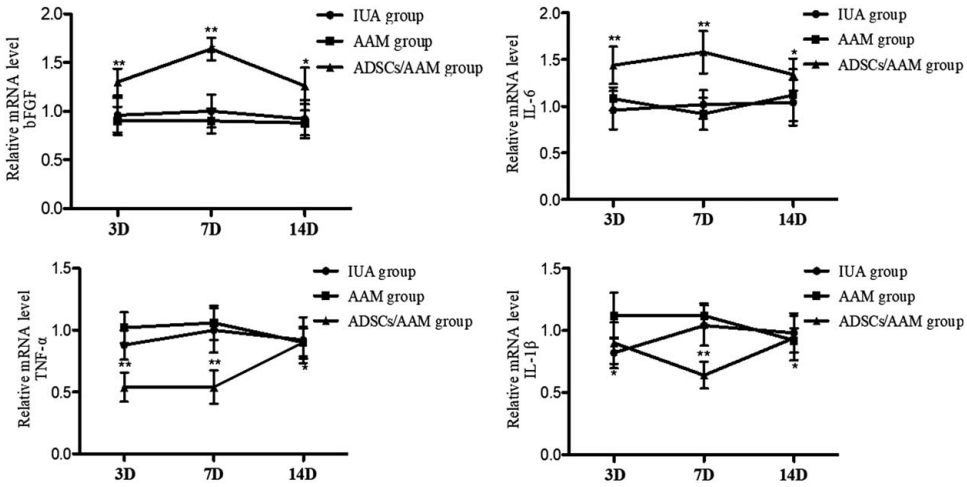


**Figure 9.** RT-PCR measurements of bFGF, IL-6, TNF-α, and IL-1β on 3, 7, and 14 days postoperatively in the sham, ADSCs/AAM, AAM, and IUA group. *$P$ value > 0.05 and **$P$ value <0.05. All results are showed as the mean ± SD of three independent experiments. AAM, acellular amniotic membrane; ADSC, adipose-derived stem cell; IUA, intrauterine adhesion.

Clinically, hysteroscopic adhesiolysis and intrauterine device placement are the standard methods for IUA treatment. However, due to the low biocompatibility of intrauterine device, they may result in inflammatory response, prevent functional endometrial regeneration, and even lead to intrauterine infections[24]. In this study, we successfully regenerated the endometrium using human AAM. After removing cellular components, AAM can serve as a natural ingredient to enhance cell adhesion, proliferation, and differentiation, making it an ideal choice for regenerative medicine[25]. As is well known, intrauterine curettage at 2–4 weeks after delivery is most likely to lead to scar formation and irreversible uterine wall damage. According to our results, AAM gradually degraded and disappeared within 7–14 days after implantation, which precisely played a preventive role in the formation of IUA. Although AAM can effectively prevent fibrotic tissue caused by endometrial damage, it is still a great challenge to promote tissue regeneration, including neovascularization, cell proliferation, and endometrial repair.

Basal ESCs are considered the source of endometrial regeneration when the endometrium shades and regenerates during each menstrual cycle[26–28]. ESCs are mainly located in the basal layer of the human endometrium, similar to adult mesenchymal stem cells[25]. It is reported that ESCs play an important role in endometrial regeneration[10,11]. However, the difficulty of obtaining ESCs limits their widespread application. Several other sources of mesenchymal stem cells for endometrial regeneration were also proposed, such as bone marrow mesenchymal stromal cells, menstrual blood-derived mesenchymal stromal cells, and amniotic tissue-derived mesenchymal stromal cells[13,29,30]. They all have a strong ability to reduce uterine fibrosis after endometrial injury. In this study, we chose ADSCs as seed cells because they are easy to obtain and rapidly expand. In order to maintain a certain number of implanted cells, we transplanted ADSCs/AAM into the uterine cavity, where ADSCs can gradually migrate to the lesion site. Compared to single AAM transplantation, ADSCs/AAM can produce thicker endometrium, more endometrial glands, and lower fibrotic area. Meanwhile, we also found that the expression levels of CD31, VEGF, E-cadherin, and vimentin in the ADSCs/AAM group were higher than those in the AAM group. These results indicated that the use of ADSCs/AAM can reduce intrauterine fibrosis and achieve the recovery of functional endometrium.

The formation of fibrosis is believed to be due to excessive deposition of ECM[31]. Sequencing data suggested that IUA was associated with immune activation and endothelial/epithelial cell development in the early stages, while in the later stages, it was highly enriched in cell–matrix adhesion[32]. When ADSCs/AAM was implanted to repair endometrial damage, RNA sequencing showed that ADSCs could regulate the immune effector process, neutrophil activation, and endocytosis, which is beneficial for reducing the immune response. According to previous reports, ADSCs can reduce the expression of pro-inflammatory cytokines, such as IL-1β, TNF-α, and IL-8, and increase the secretion of anti-inflammatory cytokines, such as IL-6 and IL-10[23–34]. ADSCs can also inhibit the excessive production of collagen by regulating inflammatory cytokines[35]. Our results indicated that ADSCs can up-regulate the expression levels of anti-inflammatory cytokines (IL-6 and bFGF) and down-regulate the expression levels of pro-inflammatory cytokines (IL-1 β and TNFα) on 3 and 7 days after surgery. However, 14 days after surgery, there was no significant difference in all inflammatory factors between the ADSCs/AAM and the AAM group, indicating that ADSCs played a role in early inhibition of inflammatory response. These phenomena partially explain the mechanism that ADSCs can maintain a relatively mild immune microenvironment. It is very beneficial for the regeneration and functional recovery of the endometrium.

A strength of this study is the high-precision scraping of the depth of the endometrial layer, which is crucial for assessing the regenerative ability of ADSCs in IUA models. However, our research has some limitations. According to our pregnancy tests, both the sham group and the ADSCs/AAM groups had high miscarriage rates. The possible reason was that the receptivity of the endometrium is impaired when the uterine cavity is opened, which is critical for embryo implantation. Multiple surgeries and possible ovarian damage were unfavorable factors for the conception and pregnancy of rats. In addition, severely damaged endometrium may also increase local inflammatory response, leading to embryo implantation failure. More importantly, the

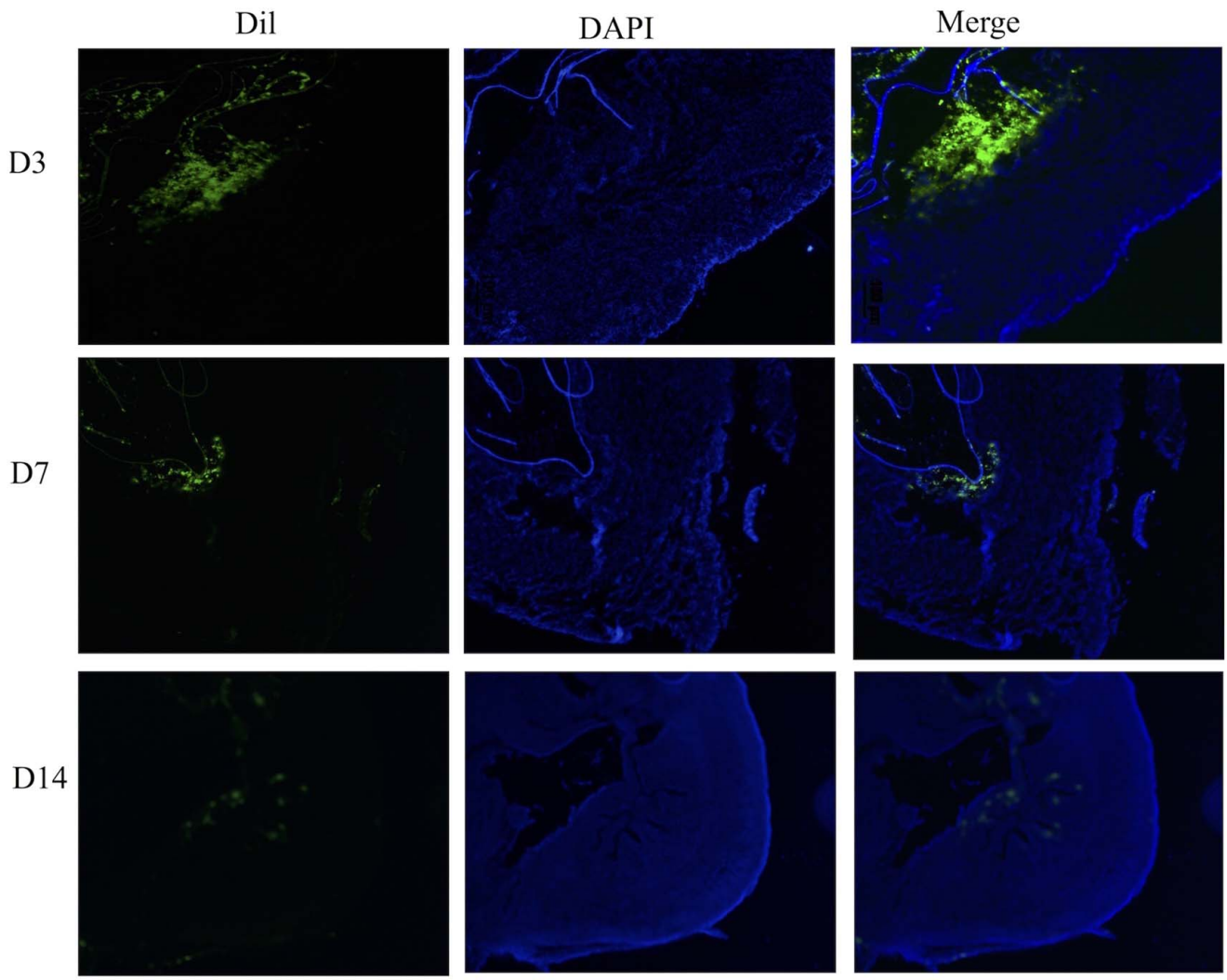


**Figure 10.** Tracking of ADSCs in vivo. Dil were used to show the presence of transplanted ADSCs. Green represents positive Dil staining, whereas blue color represents DAPI staining for nucleus. The merge image of the Dil and DAPI indicated the location of ADSCs in the regenerated endometrium. Scale bar = 200 μm. ADSC, adipose-derived stem cell.

ovarian status of the animal has not been investigated. The ovarian reserve that decreases with age can affect the possibility of gestation occurrence[36]. In addition, it is necessary to explore the appropriate timing of endometrial repair to achieve high pregnancy rates, which will be further studied. Large-scale studies should be conducted to evaluate pregnancy outcomes.

In summary, our research findings indicated that AAM loaded with ADSCs can effectively prevent the formation of fibrosis and promote endometrial regeneration. Although the exact mechanism of ADSCs in treating IUA remained unclear, our study confirmed that ADSCs can regulate the local immune microenvironment by promoting the secretion of anti-inflammatory factors and inhibiting the secretion of pro-inflammatory factors.

## Ethical approval

Ethical approval for this study (number: 2021JS-017) was provided by the Ethical Committee of The Obstetrics & Gynecology Hospital of Fudan University, Shanghai, China, on December 2021.

## Consent

Written informed consent was obtained from the patient. A copy of the written consent is available for review by the Editor-in Chief of this journal on request.

## Source of funding

The Clinical Research Plan of SHDC (SHDC2020CR1045B) to Keqin Hua; Shanghai Municipal Health commission (20194Y0085) to Chunbo Li; The Shanghai 'Rising Stars of Medical Tale' Youth Development Program (SHWSRS2020087) to Chunbo Li.

## Author contribution

Chunbo Li and Liangfeng Yao conducted most of the experiments, analyzed the data, and wrote the paper. Chunbo Li and Liangfeng Yao analyzed the data, and wrote the paper. Fengquan He reviewed and revised the paper. Fengquan He and Keqin Hua organized and submitted the manuscript. Keqin Hua guided the

whole process. All authors reviewed the results and approved the manuscript.

## Conflicts of interest disclosure

The authors declare no conflict of interest.

## Research registration unique identifying number (UIN)

Not applicable.

## Guarantor

All authors had agreed to publish the papers.

## Data availability statement

The authors confirm that the data supporting the findings of this study are available within the article.

## Provenance and peer review

Not applicable.

## Animal welfare statement

All authors confirm that (a) the present study followed international, national and/or institutional guidelines for humane animal treatment and complied with relevant legislation; (b) the present study involved client-owned animals and demonstrated a high standard (best practice) of veterinary care and involved informed client consent; or (c) guidelines for humane animal treatment did not apply to the present study.

## References


[1] Di Spiezio Sardo A, Calagna G, Scognamiglio M, *et al*. Prevention of intrauterine post-surgical adhesions in hysteroscopy. A systematic review. Eur J Obstetr Gynecol Reprod Biol 2016;203:182–92.

[2] March CM. Asherman's syndrome. Semin Reprod Med 2011;29:83–94.

[3] Guo EJ, Chung JPW, Poon LCY, *et al*. Reproductive outcomes after surgical treatment of asherman syndrome: a systematic review. Best Pract Res Clin Obstetr Gynaecol 2019;59:98–114.

[4] Robinson JK, Colimon LM, Isaacson KB. Postoperative adhesiolysis therapy for intrauterine adhesions (Asherman's syndrome). Fert Steril 2008;90:409–14.

[5] Salazar CA, Isaacson K, Morris S. A comprehensive review of Asherman's syndrome: causes, symptoms and treatment option. Curr Opin Obstet Gynecol 2017;29:249–56.

[6] Gholipourmalekabadi M, Sameni M, Radenkovic D, *et al*. Decellularized human amniotic membrane: how viable is it as a delivery system for human adipose tissue-derived stromal cells? Cell Proliferat 2016;49:115–21.

[7] Hortensius RA, Harley BA. Naturally derived biomaterials for addressing inflammation in tissue regeneration. Exp Biol Med (Maywood) 2016; 241:1015–24.

[8] Farhadihosseinabadi BF, M, Tayebi T, *et al*. Amniotic membrane and its epithelial and mesenchymal stem cells as an appropriate source for skin tissue engineering and regenerative medicine. Artif Cells Nanomed Biotechnol 2018;46:431–40.

[9] Deans R, Abbott J. Review of intrauterine adhesions. J Minim Invasive Gynecol 2010;17:555–69.

[10] Parashar S, Pajai S, Tarang T. Recent advancement in the management of intrauterine adhesions using stem cell therapy: a review article. Cureus 2023;15:e43553.

[11] Nguyen HP, Sprung CN, Gargett CE. Differential expression of Wnt signaling molecules between pre- and postmenopausal endometrial epithelial cells suggests a population of putative epithelial stem/progenitor cells reside in the basalis layer. Endocrinology 2012;153:2870–83.

[12] Liu Y, Tal R, Pluchino N, *et al*. Systemic administration of bone marrow-derived cells leads to better uterine engraftment than use of uterine-derived cells or local injection. J Cell Mol Med 2018;22:67–76.

[13] Wang J, Ju B, Pan C, *et al*. Application of bone marrow-derived mesenchymal stem cells in the treatment of intrauterine adhesions in rats. Cell Physiol Biochem 2016;39:1553–60.

[14] Shao X, Ai G, Wang L, *et al*. Adipose-derived stem cells transplantation improves endometrial injury repair. Zygote 2019;27:1–8.

[15] Kilkenny C, Browne WJ, Cuthill IC, *et al*. Improving bioscience research reporting: the ARRIVE guidelines for reporting animal research. PLoS Biol 2010;8:e1000412.

[16] Lovell-Badge R, Anthony E, Barker RA, *et al*. ISSCR guidelines for stem cell research and clinical translation: the 2021 update. Stem Cell Reports 2021;16:1398–408.

[17] Koizumi N, Inatomi T, Quantock AJ, *et al*. Amniotic membrane as a substrate for cultivating limbal corneal epithelial cells for autologous transplantation in rabbits. Cornea 2000;19:65–71.

[18] Ferrari A, Hannouche D, Oudina K, *et al*. In vivo tracking of bone marrow fibroblasts with fluorescent carbocyanine dye. J Biomed Mater Res 2001;56:361–7.

[19] Gurevich DB, David DT, Sundararaman A, *et al*. Endothelial heterogeneity in development and wound healing. Cells 2021;10:2338.

[20] Debras E, Capmas P, Maudot C, *et al*. Uterine wound healing after caesarean section: a systematic review. Eur J Obstet Gynecol Reprod Biol 2024;296:83–90.

[21] Thalla DG, Lautenschläger F. Extracellular vimentin: battle between the devil and the angel. Curr Opin Cell Biol 2023;85:102265.

[22] Piprek RP, Kloc M, Mizia P, *et al*. The central role of cadherins in gonad development, reproduction, and fertility. Int J Mol Sci 2020;21:8264.

[23] Panayotidis C, Weyers S, Bosteels J, *et al*. Intrauterine adhesions (IUA): has there been progress in understanding and treatment over the last 20 years? Gynecol Surg 2008;6:197–211.

[24] Yang JH, Chen CD, Chen SU, *et al*. The influence of the location and extent of intrauterine adhesions on recurrence after hysteroscopic adhesiolysis. BJOG 2016;123:618–23.

[25] Salah RA, Mohamed IK, El-Badri N. Development of decellularized amniotic membrane as a bioscaffold for bone marrow-derived mesenchymal stem cells: ultrastructural study. J Mol Histol 2018;49:289–301.

[26] Azizi R, Aghebati-Maleki L, Nouri M, *et al*. Stem cell therapy in Asherman syndrome and thin endometrium: Stem cell- based therapy. Biomed Pharmacother 2018;102:333–43.

[27] Gargett CE, Schwab KE, Deane JA. Endometrial stem/progenitor cells: the first 10 years. Hum Reprod Update 2016;22:137–63.

[28] Shamosi A, Mehrabani D, Azami M, *et al*. Differentiation of human endometrial stem cells into endothelial-like cells on gelatin/chitosan/bioglass nanofibrous scaffolds. Artif Cells Nanomed Biotechnol 2017;45:163–73.

[29] Zhao J, Zhang Q, Wang Y, *et al*. Uterine infusion with bone marrow mesenchymal stem cells improves endometrium thickness in a rat model of thin endometrium. Reprod Sci 2015;22:181–8.

[30] Zheng SX, Wang J, Wang XL, *et al*. Feasibility analysis of treating severe intrauterine adhesions by transplanting menstrual blood-derived stem cells. Int J Mol Med 2018;41:2201–12.

[31] Resnikoff HA, Miller CG, Schwarzbauer JE. Implications of fibrotic extracellular matrix in diabetic retinopathy. Exp Biol Med (Maywood) 2022;247:1093–102.

[32] Bazoobandi S, Tanideh N, Rahmanifar F, *et al*. Induction of Asherman's syndrome in rabbit. J Reprod Infertil 2016;17:10–6.

[33] Petrova V, Vachkova E. Outlook of adipose-derived stem cells: challenges to their clinical application in horses. Vet Sci 2023;10:348.

[34] Jahandideh S, Khatami S, Eslami Far A, *et al*. Anti-inflammatory effects of human embryonic stem cell-derived mesenchymal stem cells secretome preconditioned with diazoxide, trimetazidine and MG-132 on LPS-induced systemic inflammation mouse model. Artif Cells Nanomed Biotechnol 2018;46:1178–87.

[35] Sukho P, Cohen A, Hesselink JW, *et al*. Adipose tissue-derived stem cell sheet application for tissue healing in vivo: a systematic review. Tissue Eng Part B Rev 2018;24:37–52.

[36] Hegazy AA. Is there any mean to postpone the menopausal ovarian senescence? Int J Fertil Steril 2020;13:346–7.